Neurosci. Bull. January, 2021, 37(1):31–44
https://doi.org/10.1007/s12264-020-00519-1

www.neurosci.cn
www.springer.com/12264

ORIGINAL ARTICLE

Respiratory Control by Phox2b-expressing Neurons in a Locus Coeruleus–preBötzinger Complex Circuit

Na Liu[1,2] · Congrui Fu[3] · Hongxiao Yu[1] · Yakun Wang[1] · Luo Shi[1] · Yinchao Hao[1] · Fang Yuan[1] · Xiangjian Zhang[4] · Sheng Wang[1]

Received: 1 December 2019 / Accepted: 12 March 2020 / Published online: 28 May 2020

Abstract The locus coeruleus (LC) has been implicated in the control of breathing. Congenital central hypoventilation syndrome results from mutation of the paired-like homeobox 2b (Phox2b) gene that is expressed in LC neurons. The present study was designed to address whether stimulation of Phox2b-expressing LC ($Phox2b^{LC}$) neurons affects breathing and to reveal the putative circuit mechanism. A Cre-dependent viral vector encoding a Gq-coupled human M3 muscarinic receptor (hM3Dq) was delivered into the LC of Phox2b-Cre mice. The hM3Dq-transduced neurons were pharmacologically activated while respiratory function was measured by plethysmography. We demonstrated that selective stimulation of $Phox2b^{LC}$ neurons significantly increased basal ventilation in conscious mice. Genetic ablation of these neurons markedly impaired hypercapnic ventilatory responses. Moreover, stimulation of $Phox2b^{LC}$ neurons enhanced the activity of preBötzinger complex neurons. Finally, axons of $Phox2b^{LC}$ neurons projected to the preBötzinger complex. Collectively, $Phox2b^{LC}$ neurons contribute to the control of breathing most likely *via* an LC–preBötzinger complex circuit.

Keywords Locus coeruleus · Phox2b · Hypercapnic ventilatory response · Chemoreceptor · Neural circuit

Introduction

Congenital central hypoventilation syndrome (CCHS) is a rare genetic respiratory disease. The patients manifest obvious hypoventilation during sleep but normal or mild hypoventilation during wakefulness. More than 90% of CCHS patients carry a heterozygous mutation of the paired-like homeobox 2b (Phox2b) gene [1]. Accumulated evidence indicates that the response to hypercapnia is markedly reduced in animal models and CCHS patients, and this is most likely attributable to abnormal structure and function of central respiratory chemoreceptors [1–4]. In addition, mice carrying heterozygous mutation of Phox2b exhibit not only a reduced number of retrotrapezoid nucleus (RTN) neurons but also a blunted hypercapnic ventilatory response (HCVR) [5]. During wakefulness, both volitional and metabolic pathways are active in determining the minute ventilation (MV) necessary to maintain eucapnia; with sleep onset, the primary determinant of ventilation depends on the metabolic pathway that must recruit respiratory chemoreceptors. Interestingly, Phox2b is densely expressed in the RTN and nucleus tractus solitarius (NTS), as well as the locus coeruleus (LC), all of which are thought to be central respiratory chemoreceptor candidates [6].

Recently, several lines of experiments have demonstrated the physiological role of brainstem Phox2b-containing neurons in the control of breathing. In anesthetized

Na Liu, Congrui Fu and Hongxiao Yu have contributed equally to this work.

✉ Sheng Wang
wangsheng@hebmu.edu.cn

1 Department of Physiology, Hebei Medical University, Shijiazhuang 050017, China

2 Department of Physiology, Cangzhou Medical College, Cangzhou 061000, China

3 School of Nursing, Hebei Medical University, Shijiazhuang 050000, China

4 Hebei Key laboratory of Vascular Homeostasis and Hebei Collaborative Innovation Center for Cardio-cerebrovascular Disease, Shijiazhuang 050000, China

rodents, optogenetic stimulation of Phox2b-containing RTN neurons potentiates breathing [7]; in contrast, selective ablation of these neurons inhibits the central respiratory chemoreflex [8]. In addition, the majority of Phox2b-containing RTN neurons exhibit robust CO_2/H^+ sensitivity [9]. Our recent findings demonstrated that in conscious mice, chemogenetic stimulation of Phox2b-expressing NTS neurons produces a long-lasting increase in basal ventilation *via* a significant increase in respiratory frequency (RF) [10]; genetic ablation of these neurons significantly attenuates the HCVR [11]. Moreover, a subset of Phox2b-expressing NTS neurons also display CO_2/H^+ sensitivity *in vitro* [11]. These respiratory effects of Phox2b-expressing neurons in the RTN and NTS are reminiscent of a presumably similar role in the LC.

The LC, a noradrenergic nucleus in the pons, sends/receives widespread projections to/from many brain regions to regulate sleep/wake states, attention, and arousal [12–14], as well as breathing [15, 16]. For instance, the HCVR is significantly inhibited in rats with proportional loss of LC noradrenergic neurons, suggesting an important contribution of LC neurons to the central respiratory chemoreflex [15, 16]. Moreover, a notable loss of LC neurons occurs in CCHS patients and a Phox2b mutant mouse model [17, 18]. However, it remains incompletely understood whether activation of $Phox2b^{LC}$ neurons regulates basal pulmonary ventilation. In addition, the possible circuit mechanism underlying such an effect has not yet been determined.

Here, we used a chemogenetic approach to assess whether selective stimulation of $Phox2b^{LC}$ neurons affects basal ventilation, and to address whether $Phox2b^{LC}$ neurons are required for the HCVR. Finally, we attempted to reveal the circuit mechanism responsible for the control of breathing by $Phox2b^{LC}$ neurons.

Materials and Methods

Animals

Phox2b-Cre, Phox2b-EGFP-Jx101, and C57BL/6 J mice were used in the present study. Phox2b-Cre mice were provided by the Jackson Laboratory (Stock Number: 016223) on a C57BL/6 J genetic background. Phox2b-EGFP-Jx101 transgenic mice were supplied by the Mutant Mouse Regional Resource Center (University of California at Davis, USA) and designed by the Gene Expression Nervous System Atlas Project research group at Rockefeller University. Both mouse lines have been verified in our laboratory [10, 11]. Mice were housed at a controlled temperature and humidity under a fixed 12-h light/12-h dark cycle, with *ad libitum* access to food and water. The animal use was conducted in compliance with the Guide for the Care and Use of Laboratory Animals. The experimental protocol was approved by the Animal Care and Ethics Committee of Hebei Medical University (Hebmu-2017002).

Viral Vectors and Stereotaxic Surgery

The Cre-dependent adeno-associated viral vectors (AAVs) were from Shanghai Taitool Bioscience Co., Ltd. For surgery, male adult Phox2b-Cre transgenic mice (25 g–30 g) were anesthetized with pentobarbital sodium (60 μg/g, i.p.). Depth of anesthesia was assessed by an absence of corneal and hindpaw withdrawal reflexes. Additional anesthetic was administered as necessary (30% of the initial dose). All surgical procedures were carried out under strict aseptic conditions. After anesthesia, the mouse was placed prone on a stereotaxic apparatus (RWD Life Science Co., Ltd, Shenzhen, China) and body temperature was maintained at 37°C using a heating pad and a blanket. After shaving and cleaning the skin, an incision was made to expose the skull, and then small holes were drilled over the LC region. Viral vectors were bilaterally microinjected into the LC (stereotaxic coordinates: – 5.3 mm from bregma, ± 0.8 mm lateral from midline, and – 4.0 mm vertical from cortical surface) *via* a glass micropipette connected to a syringe pump (Harvard Apparatus, Holliston, MA) based on the Mouse Brain in Stereotaxic Coordinates [19]. The pipette was retained *in situ* for at least 5 min after injections to allow sufficient diffusion of virus. After surgery, the mice received injections of ampicillin (125 mg/kg, i.p.) and the analgesic ketorolac (4 mg/kg, i.p.). Mice were caged individually and given 4 weeks to recover before breathing measurements and histological experiments.

Chemogenetic Stimulation and Breathing Measurements

The protocol for chemogenetic stimulation has been described in detail [10]. Shortly, a Cre-dependent viral vector (AAV-EF1α-DIO-hM3Dq-mCherry; titer, 10^{12} virus molecules per milliliter; 100 nL per injection; total volume: 200 nL) encoding a gene cassette for expression of a mutated human Gq-coupled M3 muscarinic receptor (hM3Dq), a type of designer receptor exclusively activated by designer drugs (DREADD), was microinjected into the LC region based on the above stereotaxic coordinates. An equal volume of the control vector AAV-EF1α-DIO-mCherry (titer, 10^{12}/mL) was also microinjected. Four weeks after virus injections, breathing parameters were measured in conscious, freely-moving mice by whole-body plethysmography (EMKA Technologies, Paris, France) as

previously described [10]. Briefly, mice were allowed to adapt to a recording chamber for at least 2 h before the testing protocol. Mice were exposed to room air (21% O_2) throughout experiments. A mass flow regulator provided quiet, smooth, and constant flow through the recording chamber (0.5 L/min). Air-flow signals were recorded, amplified, digitized, and analyzed using IOX software (EMKA Technologies) to determine breathing parameters over sequential 20 s epochs (about 50 breaths) during periods of behavioral quiescence and regular breathing. The breathing parameters RF (breaths/min), tidal volume (TV, μL/g), and MV (μL/g per minute), were consecutively collected and read out in a real-time mode. MV was calculated as the product of RF and TV, normalized to body weight (g). For chemogenetic stimulation of $Phox2b^{LC}$ neurons, clozapine-N-oxide (CNO, 1 mg/kg), an activator of hM3Dq, was intraperitoneally injected into hM3Dq-transduced mice and breathing parameters were continuously collected for 4 h. At the end of the experiments, mice were sacrificed with an overdose of pentobarbital and transcardially perfused for histology.

Assessment of HCVR

The microinjection protocol was used as described above. For genetic ablation of $Phox2b^{LC}$ neurons, the Cre-dependent AAV vector encoding a genetically-engineered Casp3 gene (AAV-CAG-DIO-taCasp3-TEVp; titer, 10^{13}/mL; 50 nL per injection; total volume: 100 nL) or an equal volume of control vector (AAV-CAG-DIO-mCherry) was bilaterally microinjected into the LC of Phox2b-Cre mice. To verify ablation of $Phox2b^{LC}$ neurons, quantitative PCR (qPCR) was performed as described previously [10]. In brief, after anesthesia, the LC tissue was rapidly dissected out and placed in lysate solution, followed by reverse transcription (Super Script III First-Strand Synthesis System, ThermoFisher Scientific, Waltham, MA, USA). The products were amplified and analyzed using the ABI Quant Studio 6 flex system (1 cycle at 50°C for 2 min; 1 cycle at 95°C for 2 min; 40 cycles at 95°C for 10 s, 60°C for 30 s, and 72°C for 1 min). GAPDH was used as an internal reference. The following primers were used: GAPDH forward: 5′-GCAAATTCAACGGCACAGTCAAGG-3′, reverse: 5′-TCTCGTGGTTCACACCCATCACAA-3′; Phox2b forward: 5′-TACGCCGCAGTTCCATACAAACTC-3′, reverse: 5′-TCTTTGAGCTGCGCGCTTGTGAAG-3′. The HCVR was assessed 4 weeks after vector microinjection. For analysis of the HCVR, mice were sequentially exposed to 100% O_2, 2% CO_2, 5% CO_2, and 8% CO_2 for 7 min (balanced O_2; each separated by 5 min of 100% O_2). The peak value of each breathing parameter in response to different concentrations of CO_2 was calculated using 60 s epochs (about 150 breaths). Hypercapnic exposure was conducted under the condition of hyperoxia to largely reduce the contribution of peripheral chemoreceptors to the HCVR.

Histology

The immunofluorescence protocol has been described [10]. In brief, under deep anesthesia with urethane (1.8 g/kg, i.p.), mice were perfused transcardially with 50 mL cold saline, followed by 4% phosphate-buffered paraformaldehyde (pH 7.4). Each mouse was decapitated and the brainstem was dissected out, stored in 4% perfusion fixative at 4°C for 24 h–48 h, and then immersed in 30% sucrose in phosphate-buffer saline (PBS) for at least 2 days. Coronal sections were cut at 25 μm on a freezing cryostat (CM1950; Leica Microsystems, Germany) and blocked for 1 h at room temperature in 5% BSA with 0.25% Triton X-100 in PBS. Sections were incubated with primary antibodies against Phox2b (1:200, sc-376997; Santa Cruz Biotechnology, Inc., Santa Cruz, CA), tyrosine hydroxylase (TH, 1:1000, AB152; Millipore, Billerica, MA, USA), cFos (1:400, #2250; Cell Signaling Technology, Danvers, MA), or EGFP (1:1000, ab13970; Abcam, Cambridge, MA) overnight at 4°C. After rinsing with PBS for 15 min, appropriate fluorescently-conjugated secondary antibodies were applied for 1 h at room temperature, followed by rinsing with PBS again. Finally, the sections were mounted on slides with Vectashield Antifade Mounting Medium (Vector Laboratories, Burlingame, CA) and visualized using a fluorescence (DM6000B, Leica, Germany) or confocal microscope (LSM800, Carl Zeiss, Germany). Note that the Phox2b antibody was validated in our prior studies [10, 11].

For cFos-based histological analysis of CNO-stimulated LC neurons, the hM3Dq-transduced mice exposed to room air were injected with CNO (1 mg/kg, i.p.) or an equal volume of saline. After 120 min, each mouse was anesthetized and perfused transcardially with fixative for subsequent histological processing. For cFos-based evaluation of the proportion of CO_2-activated mCherry-transduced LC neurons, each mouse was placed in a chamber and exposed to 100% O_2 or 8% CO_2 (balance O_2) for 50 min, followed by 100% O_2 for 60 min, followed by histological examination. To calculate the proportion of CO_2- or CNO-stimulated mCherry-transduced neurons in the LC, cells were counted in 6 coronal sections from each mouse. The rostrocaudal location of each section was determined (bregma: – 5.26 mm to – 5.80 mm) according to the Mouse Brain in Stereotaxic Coordinates [19]. For cFos-based analysis of whether chemogenetic stimulation of $Phox2b^{LC}$ neurons affected the neuronal activity in the preBötzinger complex (preBötC), transcardial perfusion and histological protocols were performed 120 min after injection of CNO or

saline in hM3Dq-transduced mice. To count putative cFos-expressing preBötC neurons, 5 consecutive coronal sections (bregma: – 6.72 mm to – 7.20 mm, each separated by 90 μm) were collected for histology. The Phox2b staining was conducted together with cFos to easily locate the preBötC contour. Cells were counted manually on a fluorescence or confocal microscope to obtain the total number of labeled neurons of interest.

Tracing of Phox2b^{LC} Neurons

To determine whether the axons of Phox2b^{LC} neurons project to the preBötC, the anterograde tracing virus AAV-EF1α-DIO-mCherry (titer, 10^{12}/mL; 100 nL per injection; total volume: 200 nL) was bilaterally microinjected into the LC of Phox2b-Cre mice. After successful transduction of mCherry, histological examination was carried out to check the distribution of Phox2b^{LC} neuronal axons in the preBötC. For retrograde tracing of Phox2b^{LC} neurons, AAV_{retro}-EF1α-DIO-EGFP (titer, 10^{13}/mL; 50 nL per injection; total volume: 100 nL) was microinjected into the preBötC of Phox2b-Cre mice (bregma coordinates: anteroposterior, – 6.8 mm; mediolateral, ± 1.2 mm; dorsoventral, – 4.65 mm). Four weeks after microinjection, EGFP-expressing neurons were visualized in the LC using a confocal microscope (Zeiss LSM800, Germany). EGFP-labeled neurons were manually counted in 6 sections from 9 mice (bregma: – 5.26 mm to – 5.80 mm, each separated by 90 μm).

Statistics

Statistical analysis was performed using Prism 8 (GraphPad, La Jolla, CA). All data are presented as the mean ± SEM. Two-group comparisons were analyzed using two-tailed Student's *t* test. The differences among groups were compared using two-way ANOVA with Bonferroni's *post hoc* test. Differences with $P < 0.05$ were considered statistically significant.

Results

Expression of Phox2b in LC Neurons

To validate the presence of Phox2b in LC neurons in adult mice, immunofluorescence staining was used in C57BL/6 J and Phox2b-EGFP mice. Here, we checked the co-expression of Phox2b and TH (a specific marker of LC neurons [20]). To that end, the immunoreactivity for Phox2b (Phox2b$^+$) and TH (TH$^+$) was examined in C57BL/6 J mice ($n = 7$) and both markers were found to be co-localized in most of the LC neurons (Fig. 1A). Based on the cell counts, Phox2b$^+$TH$^+$ neurons (643 ± 32) accounted for approximately 50% of total number of TH$^+$ neurons (1274 ± 66). In addition, using the Phox2b-EGFP mouse line, it has been reported that a large number of EGFP-expressing neurons are Phox2b$^+$ in the NTS, RTN, and LC [9, 11, 21]. Here, co-expression of TH (red) and EGFP (green) was also confirmed in adult Phox2b-EGFP mice (Fig. 1B). Altogether, these data confirm the presence of Phox2b in LC neurons in adult mice.

Validation of the Chemogenetic Approach

The chemogenetic approach has been widely used to manipulate specific cell types and modulate rodent behavior [10, 22]. Here, to selectively stimulate Phox2b^{LC} neurons, a Cre-inducible AAV vector encoding hM3Dq-mCherry was bilaterally microinjected into the LC of Phox2b-Cre mice (Fig. 2A), followed by immunofluorescence staining for validation. As shown in Fig. 2B, cell counts were obtained from each mouse ($n = 5$), and the number of neurons with immunoreactivity for both mCherry and Phox2b (mCherry$^+$Phox2b$^+$) accounted for approximately 92% of the total mCherry$^+$ neurons and for approximately 50% of the total Phox2b$^+$ neurons (Fig. 2C, D), showing that a large number of hM3Dq-mCherry-transduced neurons were Phox2b$^+$. To further determine the selective activation of Phox2b^{LC} neurons, hM3Dq-transduced mice in an awake state were injected with CNO or an equal volume of saline, followed by tissue fixation and immunohistochemical staining (Fig. 3A). cFos-immunoreactive neurons (cFos$^+$) represented the activation of Phox2b^{LC} neurons. Clearly, according to the cell counts, the number of cFos$^+$mCherry$^+$ neurons in CNO-injected mice was greater than that in saline-injected mice (192 ± 25 *versus* 22 ± 8, CNO *vs* saline, $n = 4$ for each group, $P < 0.001$, Fig. 3B, C). Hence, CNO was able to selectively activate most of the Phox2b^{LC} neurons.

Chemogenetic Activation of Phox2b^{LC} Neurons Increases Basal Ventilation

Next, we performed a gain-of-function experiment using chemogenetics to test the effect of Phox2b^{LC} neuronal stimulation on respiratory function in conscious mice. Four weeks after viral injections, whole-body plethysmography (Fig. 4A) was used to measure the respiratory parameters RF, TV and MV during exposure to room air in the CNO and saline groups. Intraperitoneal injection of CNO produced a long-lasting increase in RF (Fig. 4B) and MV (Fig. 4D), with an insignificant change in TV (Fig. 4C). The RF markedly increased 45 min after CNO injection, remained elevated for approximately 105 min and gradually declined to the control level after 150 min (162 ± 7 *vs*

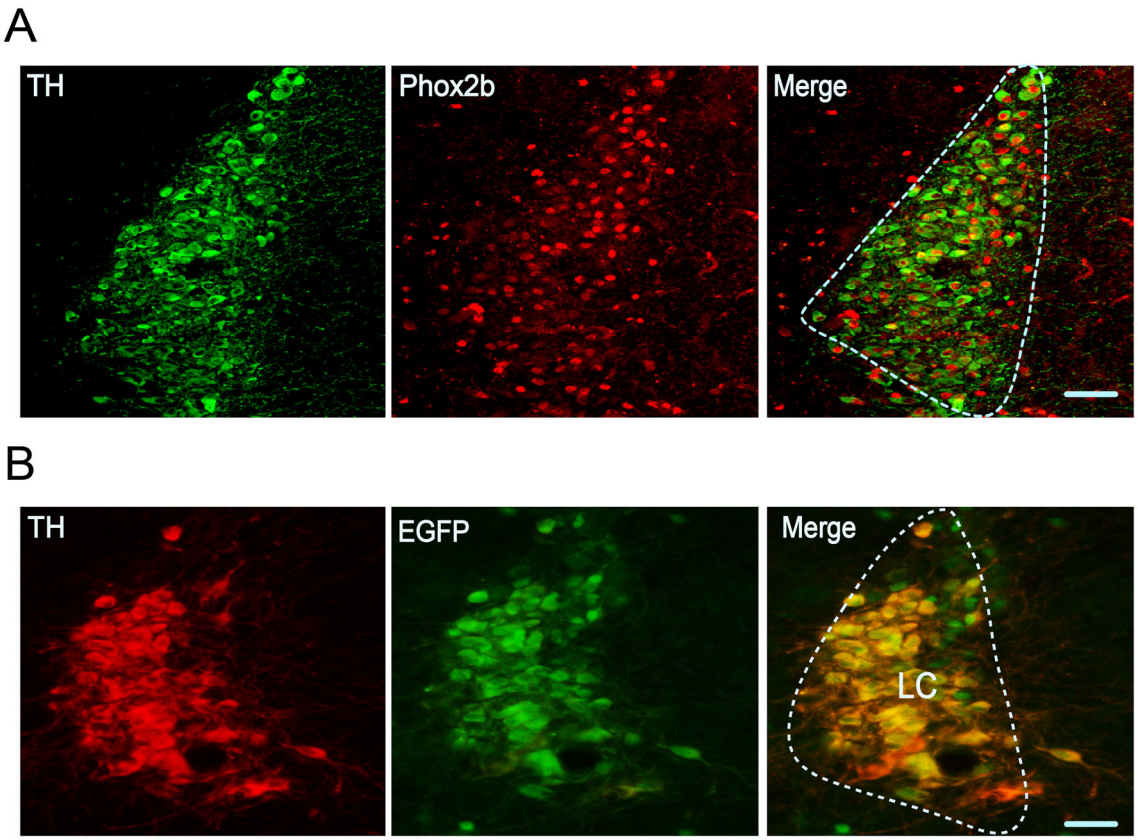

Fig. 1 Expression of Phox2b in LC neurons. Photomicrographs showing the co-expression of TH and Phox2b in LC neurons from adult C57BL/6 J (**A**) and Phox2b-EGFP (**B**) mice. The contour of LC is roughly indicated by dashed lines. Scale bars, 50 μm.

116 ± 8 breaths/min, CNO *vs* saline at approximately 75 min, $P < 0.0001$; Fig. 4B). Similarly, compared with the saline injection, the CNO injection generated a similar increase in MV, which persisted for approximately 105 min (1767 ± 82 *vs* 1168 ± 72 μL/g per minute, CNO *vs* saline at approximately 75 min, $P < 0.0001$, Fig. 4D). Administration of saline resulted in no significant increases in any breathing parameter. In control vector-injected mice (mCherry expression only), neither CNO nor saline injections caused significant changes in breathing parameters (data not shown). Collectively, we concluded that activation of Phox2b^{LC} neurons significantly increases the basal ventilation *via* an increase in RF rather than TV.

Chronic Ablation of Phox2b^{LC} Neurons Attenuates the HCVR

LC neurons have been thought to serve as a central respiratory chemoreceptor candidate [3, 23]. To further determine the role of Phox2b^{LC} neurons in the regulation of the HCVR, a loss-of-function experiment was carried out by ablation of Phox2b^{LC} neurons using a genetic approach as previously reported [10, 24]. As shown in Fig. 5A, the AAV-CAG-DIO-taCasp3-TEVp (AAV-CAG-DIO-mCherry for control) was bilaterally microinjected into the LC of Phox2b-Cre mice 4 weeks before breathing measurement. First, the effectiveness of Phox2b^{LC} neuron ablation was assessed using the unilateral injection of Casp3-containing virus into the LC, the other side being intact. The number of Phox2b^{LC} neurons on the injected side was lower than that on the control side (Fig. 5B). Quantitative analysis demonstrated that the Phox2b mRNA level in LC neurons from Casp3-transduced mice decreased by approximately 40% compared with that from mCherry-transduced mice (Fig. 5C). After validation of Phox2b^{LC} neuron ablation, we then tested the effect of bilateral ablation of Phox2b^{LC} neurons on the HCVR. Mice were sequentially exposed to 100% O_2, 2% CO_2, 5% CO_2, and 8% CO_2 and the breathing parameters were measured. During exposure to 100% O_2 and 2% CO_2, no statistical differences in RF, TV, and MV were found between the two groups. During exposure to 5% CO_2, ablation of Phox2b^{LC} neurons significantly reduced the TV and MV but not RF compared with the control group (TV: 10.0 ± 0.4 *vs* 13.9 ± 0.7 μL/g, $P < 0.0001$; MV: 2258 ± 90 *vs* 3266 ± 209 μL/g per minute, $P < 0.001$, Casp3 *vs* mCherry group, $n = 11$ for Casp3, $n = 9$ for mCherry; Fig. 5E). When 8% CO_2 was inhaled, RF, TV,

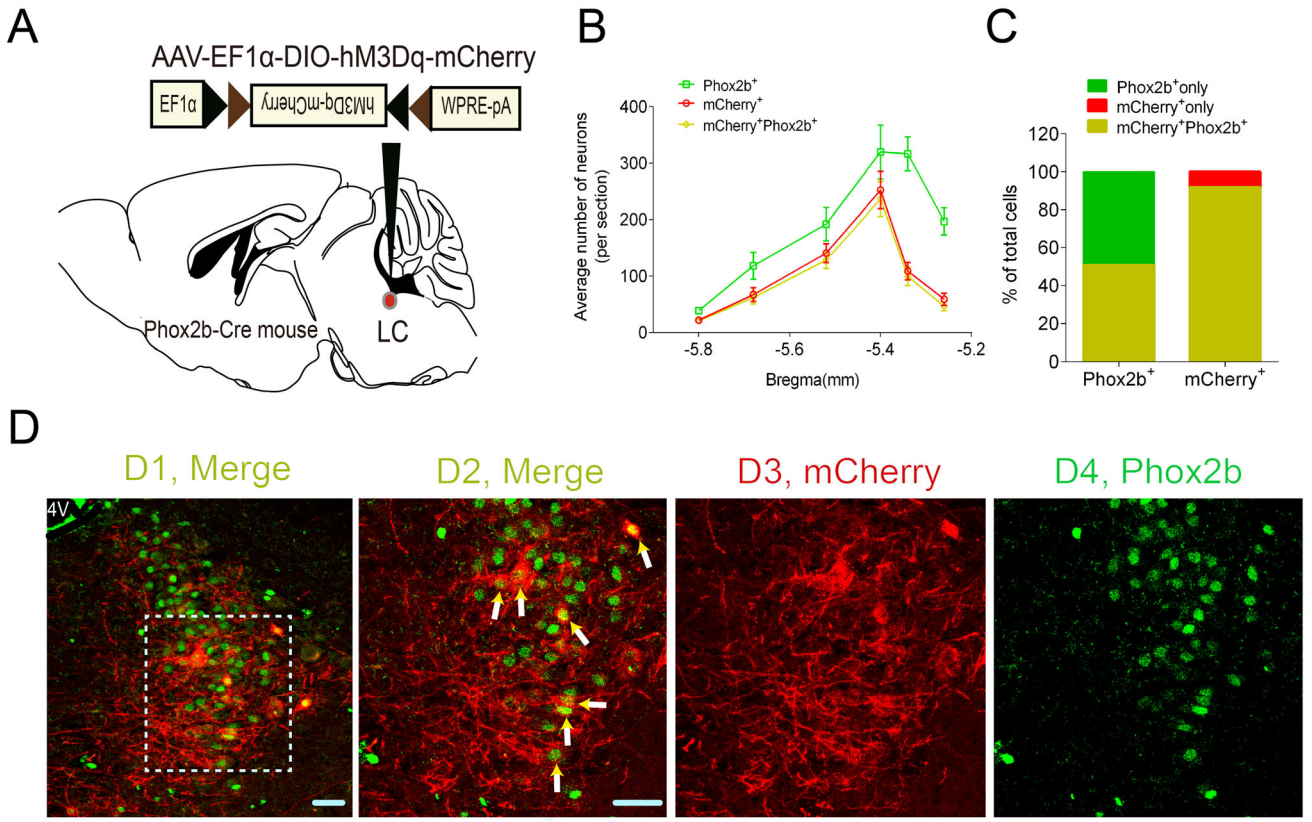

Fig. 2 Validation of hM3Dq-mCherry expression in Phox2b-Cre mice. **A** Schematic diagram showing the microinjection of viral vectors encoding hM3Dq-mCherry into the LC of Phox2b-Cre mice. **B** Rostrocaudal distribution of $Phox2b^+$, $mCherry^+$ and $mCherry^+$ $Phox2b^+$ neurons in the LC. Bilateral cell counts from 6 coronal sections (25 μm) from each mouse (n = 5). **C** Numbers of $mCherry^+Phox2b^+$ neurons account for approximately 92% of the total number of $mCherry^+$ neurons and for approximately 50% of $Phox2b^+$ neurons. **D1–4** Representative images of co-expression of Phox2b and mCherry. **D2** Enlargement of outlined area in D1. Arrows indicate $mCherry^+Phox2b^+$ neurons. **D3**, **4** Immunoreactivity for mCherry (red) and Phox2b (green). Scale bars, 50 μm; 4 V, fourth ventricle.

and MV all clearly decreased (RF: 257 ± 5 *vs* 281 ± 9 breaths/min, $P < 0.05$; TV: 13.5 ± 0.6 *vs* 18.1 ± 1.2 μL/g, $P < 0.0001$; MV: 3474 ± 188 *vs* 5093 ± 366 μL/g per minute, $P < 0.0001$; Casp3 *vs* mCherry group; Fig. 5F). Therefore, proportional ablation of $Phox2b^{LC}$ neurons significantly attenuated the HCVR.

CO_2 Sensitivity of $Phox2b^{LC}$ Neurons

The role of $Phox2b^{LC}$ neurons in the HCVR is associated with the intrinsic sensitivity to CO_2/H^+. To address whether $Phox2b^{LC}$ neurons exhibit CO_2 sensitivity, Phox2b-Cre mice injected with the AAV-EF1α-DIO-mCherry were exposed to 100% O_2 and 8% CO_2 and the immunoreactivity to cFos was examined to denote CO_2-activated cells. Fig. 6A shows immunofluorescence images of mCherry and cFos expression in the LC. The number of $cFos^+mCherry^+$ neurons was greater in mice treated with 8% CO_2 than with 100% O_2 (49 ± 4 *vs* 10 ± 1, 8% CO_2 *vs* 100% O_2, n = 3 per group, $P < 0.01$; Fig. 6B, C). Normalized data showed that $cFos^+mCherry^+$ neurons stimulated with 8% CO_2 accounted for approximately 18% of all $cFos^+$ neurons and for approximately 17% of all $mCherry^+$ neurons (Fig. 6D). These data suggest that a subgroup of $Phox2b^{LC}$ neurons is activated by CO_2 and most likely participates in the HCVR.

Stimulation of $Phox2b^{LC}$ Neurons Activates preBötC Neurons

preBötC neurons are the kernel of the respiratory central pattern generator (rCPG) [25]. It has been speculated that central respiratory chemoreceptors contribute to the control of breathing by activating the rCPG [25–27]. Therefore, we sought to address whether the stimulation of $Phox2b^{LC}$ neurons enhances the activity of preBötC neurons as represented by cFos-immunoreactivity. When hM3Dq-mCherry was successfully transduced into $Phox2b^{LC}$ neurons, CNO or saline was injected intraperitoneally, followed by immunofluorescence staining. Cell counts in 5

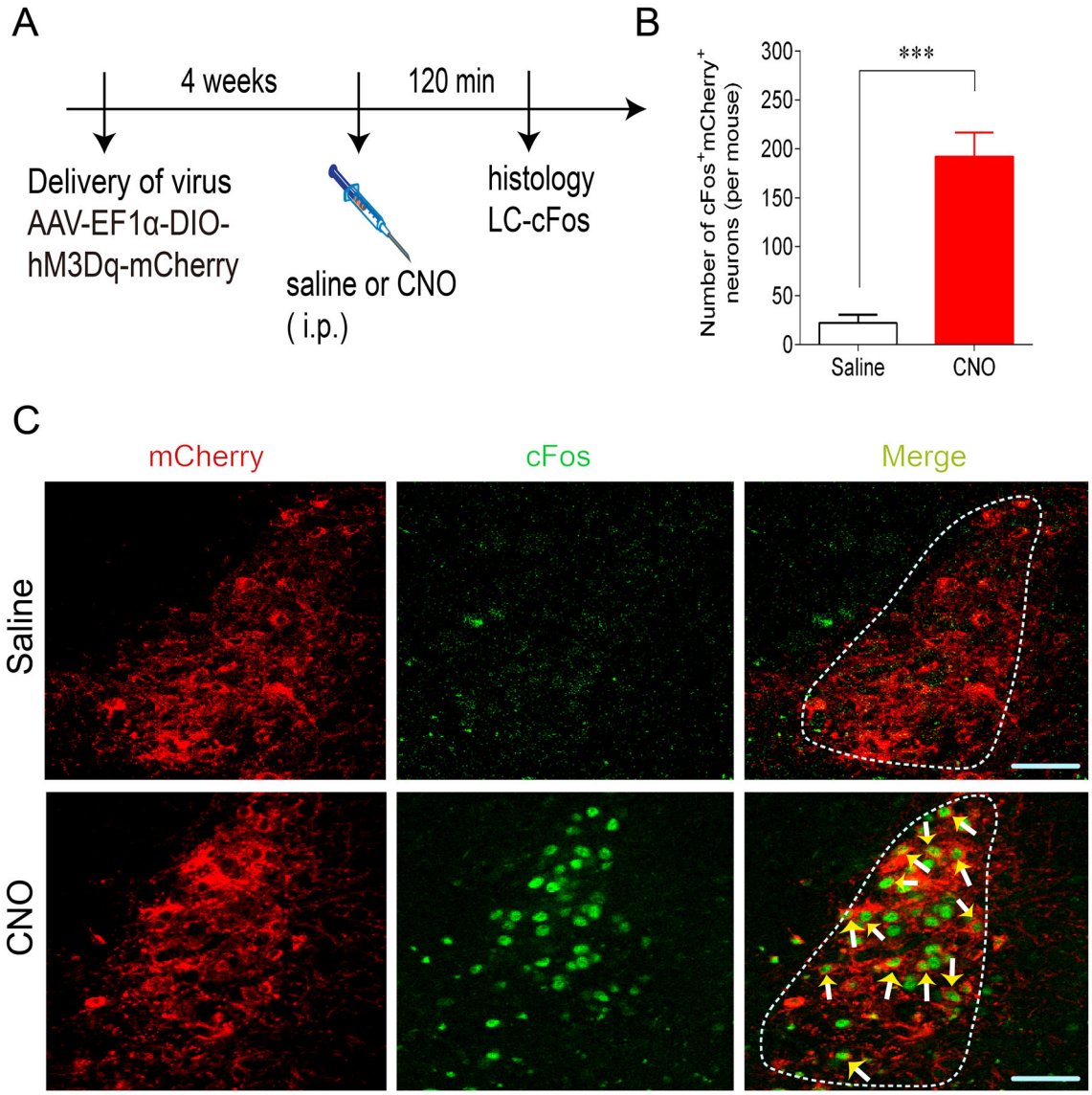

Fig. 3 Histomolecular verification of Phox2b^{LC} neuron activation. **A** Schematic of infection of Phox2b-Cre mice with AAV-EF1α-DIO-hM3Dq-mCherry by intraperitoneal injection of CNO or saline. **B** Numbers of cFos^{+}mCherry^{+} neurons in CNO (1 mg/kg)-injected mice relative to saline-injected mice. Cell counts are from 6 coronal sections from each mouse (n = 4 per group) (***$P < 0.001$, unpaired t test). **C** Representative photomicrographs showing mCherry^{+} (red) and cFos^{+} (green) neurons in the LC. Immunoreactivity for cFos indicates CNO-activated neurons (arrows). Scale bars, 50 µm.

coronal sections per mouse showed that the number of cFos^{+} neurons in the preBötC was greater in the CNO group than in the saline group (100 ± 7 *vs* 33 ± 2, CNO *vs* saline, $P < 0.001$, Fig. 7B, C). Note that due to a lack of adequately specific markers, cFos-labeled neurons were chosen based on the anatomically defined preBötC. Nevertheless, the present results suggest that stimulation of Phox2b^{LC} neurons can activate putative preBötC neurons.

Projection of Phox2b^{LC} Neurons to the preBötC

Having confirmed activation of the downstream preBötC neurons by Phox2b^{LC} neurons, we then attempted to dissect a putative direct pathway between the LC and preBötC. First, AAV-EF1α-DIO-mCherry was injected into the LC of Phox2b-Cre mice to map the axonal projection of Phox2b^{LC} neurons (Fig. 8A); immunofluorescence images demonstrated a dense distribution of putative axon terminals in the preBötC region (Fig. 8B). Because the viral vector used for anterograde tracing does not act transsynaptically [28], it can be concluded that these axons in

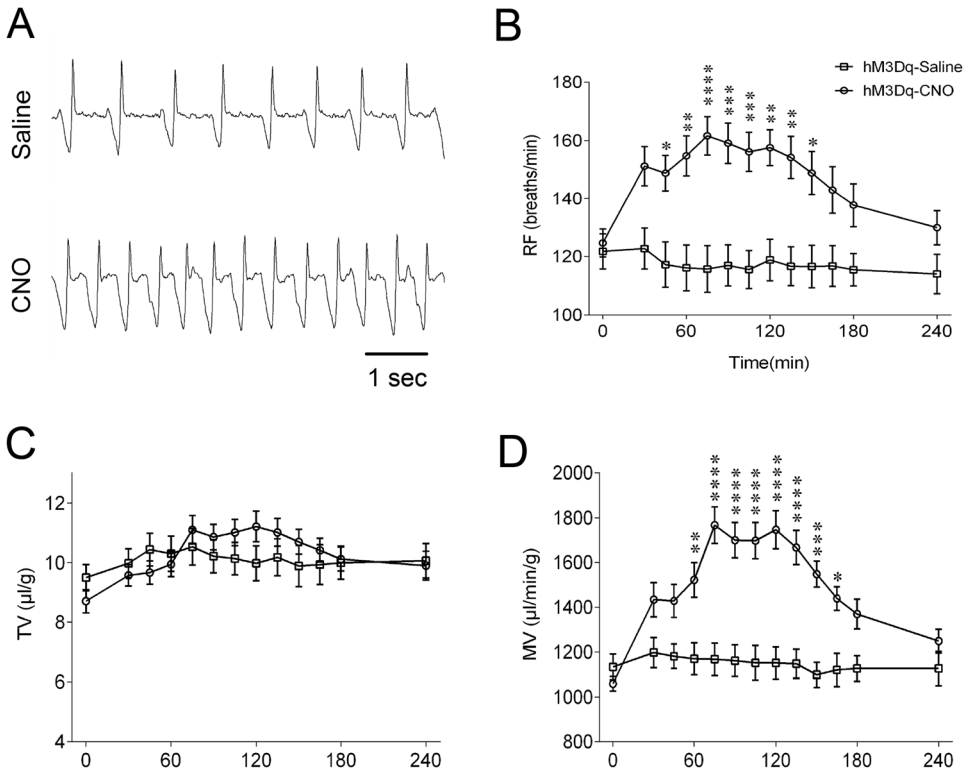

Fig. 4 Chemogenetic stimulation of Phox2b^{LC} neurons increases basal ventilation. **A** Typical traces of respiratory flow recording from hM3Dq-transduced Phox2b-Cre mice with intraperitoneal injection of saline or CNO. **B–D** Effects of Phox2b^{LC} neuron stimulation on breathing parameters. Administration of CNO, but not saline, produced marked increases in RF (**B**) and MV (**D**) but not TV (**C**) (n = 15 for saline group, n = 24 for CNO group; $^{*}P < 0.05$, $^{**}P < 0.01$, $^{***}P < 0.001$, $^{****}P < 0.0001$, saline *vs* CNO, two-way ANOVA with Bonferroni's *post hoc* test).

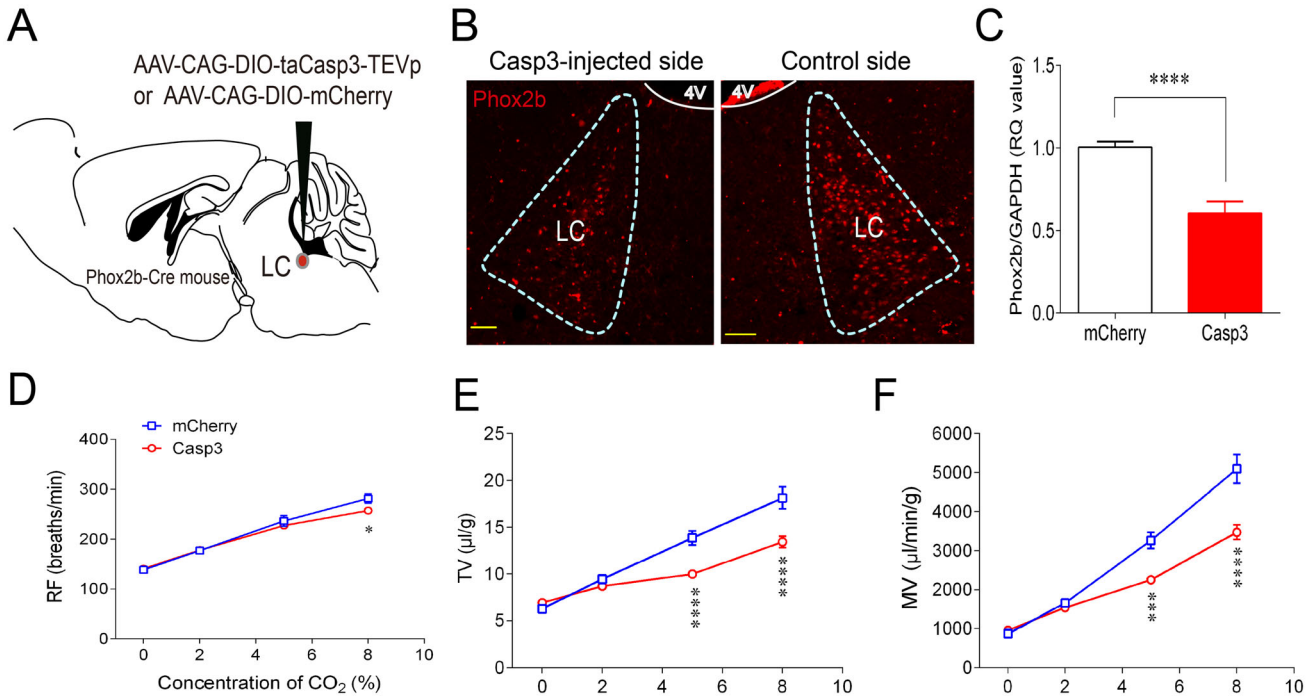

Fig. 5 Ablation of Phox2b^{LC} neurons impairs the HCVR. **A** Schematic diagram illustrating the microinjection of AAV-CAG-DIO-taCasp3-TEVp or AAV-CAG-DIO-mCherry (control virus) into the LC of Phox2b-Cre mice. **B** Immunofluorescence images showing that the number of Phox2b^{LC} neurons in the Casp3-injected side was significantly reduced compared to the control side of the LC in the same mouse (4 V, fourth ventricle; scale bars, 50 μm). **C** qPCR results for the levels of Phox2b mRNA in Casp3-transduced mice relative to mCherry-transduced mice (n = 14 samples from 7 mice for mCherry group, n = 10 samples from 5 mice for Casp3 group; $^{****}P < 0.0001$, unpaired t test). **D–F** Effects of bilateral ablation of Phox2b^{LC} neurons on breathing parameters during exposure to different concentrations of CO_2 (n = 9 for mCherry group, n = 11 for Casp3 group; $^{*}P < 0.05$, $^{***}P < 0.001$, $^{****}P < 0.0001$, two-way ANOVA with Bonferroni's *post hoc* test).

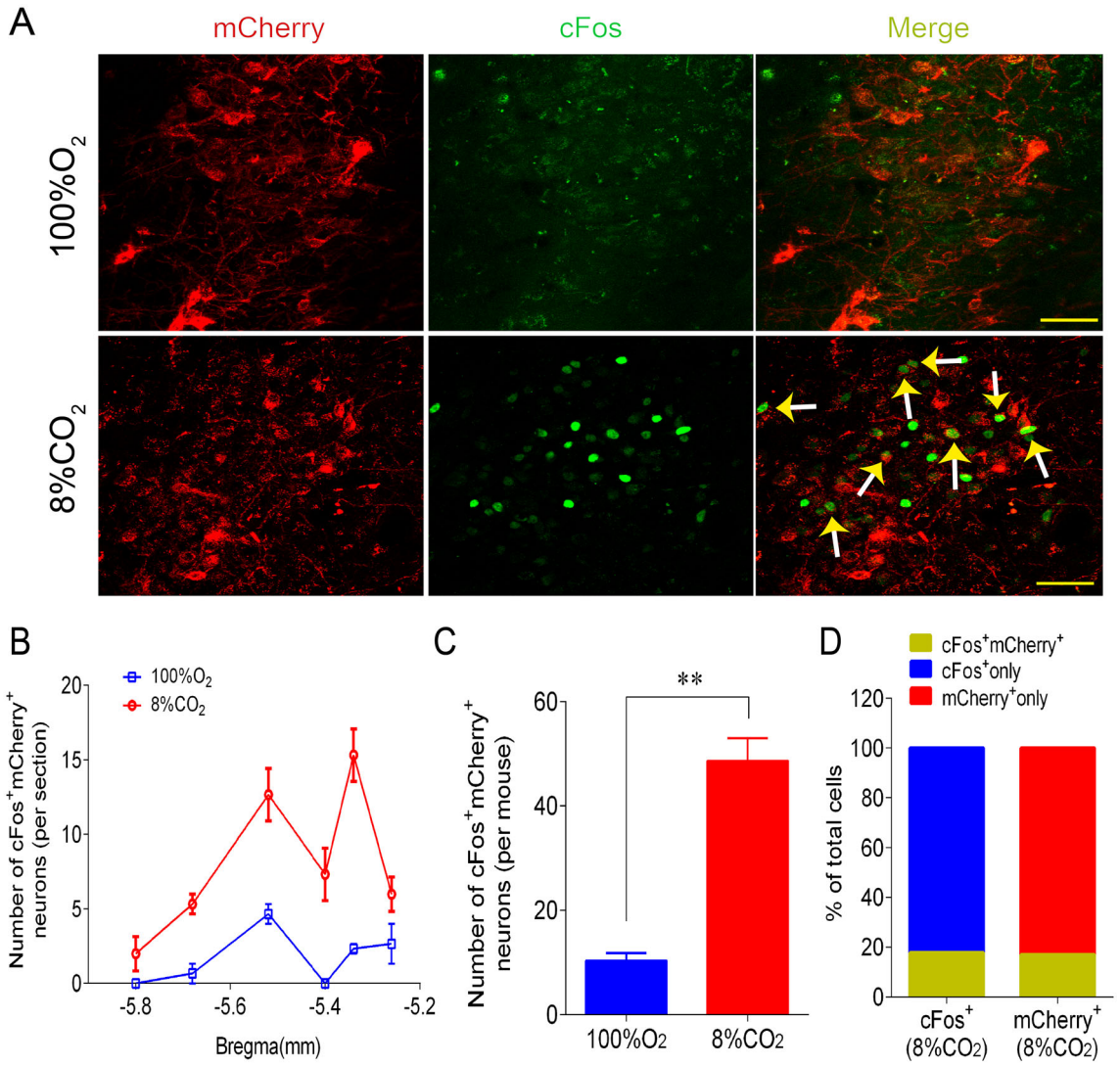

Fig. 6 CO_2 sensitivity of Phox2b^{LC} neurons. **A** Photomicrographs showing cFos$^+$ and mCherry$^+$ LC neurons in mCherry-injected mice exposed to 100% O_2 or 8% CO_2; immunoreactivity for cFos represents CO_2-activated neurons (arrows indicate mCherry$^+$cFos$^+$ neurons; scale bars, 50 μm). **B** Rostrocaudal distribution of cFos$^+$mCherry$^+$ neurons (6 coronal sections per mouse; n = 3 mice per group). **C** Numbers of cFos$^+$mCherry$^+$ neurons in mice exposed to 8% CO_2 and 100% O_2 (**$P < 0.01$, unpaired t test). **D** Percentages of cFos$^+$mCherry$^+$ neurons in the total number of cFos$^+$ and mCherry$^+$ neurons when challenged by 8% CO_2.

the preBötC originated from the somata of Phox2b^{LC} neurons. Second, AAV$_{retro}$-EF1α-DIO-EGFP, which is a retrograde tracer that infects neurons through axon terminals, was injected into the preBötC in Phox2b-Cre mice 4 weeks before histological examination (Fig. 8C); some EGFP-labeled neuronal somata, which projected axons to the preBötC, were found in the LC (Fig. 8D). Based on cell counts, EGFP$^+$Phox2b$^+$ neurons accounted for > 84% of the total number of EGFP$^+$ neurons (Fig. 8E). These data provide neuroanatomical evidence for an LC–preBötC pathway by which activation of Phox2b^{LC} neurons may increase pulmonary ventilation and HCVR.

Discussion

Noradrenergic neurons in the LC are thought to be central respiratory chemoreceptor candidates and they provide a CO_2-dependent excitatory drive to respiratory networks. However, the circuit mechanism underlying such an effect remains to be defined. In this paper, we used a chemogenetic approach in a transgenic mouse model to demonstrate that selective activation of Phox2b-expressing neurons, a putative subgroup of noradrenergic neurons in the LC, produced a long-lasting increase in basal MV *via* an increase in RF rather than TV in conscious mice. In addition, we used a genetic approach to proportionally ablate Phox2b^{LC} neurons, which resulted in an impaired

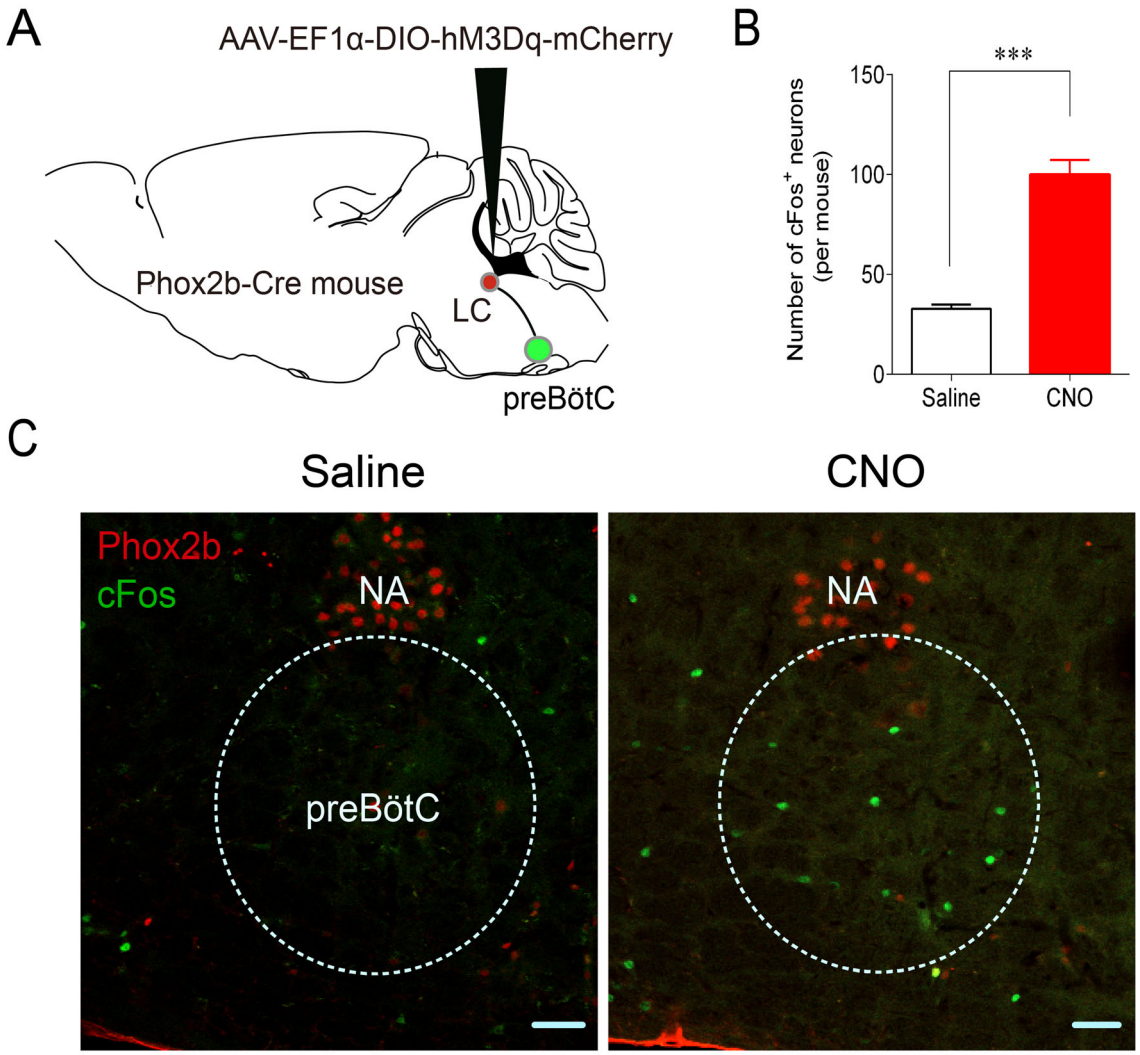

Fig. 7 Effect of Phox2b^{LC} neuron stimulation on the activity of preBötC neurons. **A** Schematic of microinjection of virus into the LC. After successful transduction of hM3Dq-mCherry in Phox2b^{LC} neurons, CNO or saline was intraperitoneally injected 2 h before histological examination for cFos labeling. **B** Numbers of cFos^{+} neurons in the preBötC in the CNO-injected and saline-injected groups (n = 4 for saline group, n = 6 for CNO group; ***$P < 0.001$, unpaired t test). **C** Photomicrographs showing cFos^{+} neurons (green) in mice treated with saline or CNO. The NA neurons were labeled by Phox2b (red). NA, nucleus ambiguus; scale bars, 50 μm.

HCVR. This phenomenon was most likely due to the CO_2-activation of a subset of Phox2b^{LC} neurons. Finally, an anatomically-defined LC–preBötC pathway is suggested to mediate the above effect of Phox2b^{LC} neurons.

Activation of Phox2b^{LC} Neurons Increases Basal Ventilation

In the present study, selective stimulation of Phox2b^{LC} neurons significantly increased basal pulmonary ventilation. This is supported by the following evidence. First, although the expression of Phox2b in adult rodents remains controversial [29, 30], our data, using Phox2b-Cre and Phox2b-EGFP mouse lines that have been validated, in combination with prior observations [6, 31], provide convincing evidence of Phox2b expression in the LC. Second, we found that > 90% of hM3Dq-transduced LC neurons were Phox2b^{+}, in favor of a significant contribution of Phox2b^{LC} neurons. Third, the majority of hM3Dq-expressing Phox2b^{LC} neurons were clearly activated by CNO. Of note, in addition to affecting breathing, stimulation of Phox2b^{LC} neurons probably had other biological effects that were not tested here, but this does not exclude the possibility that stimulation of non-Phox2b^{LC} neurons increases basal ventilation.

Interestingly, gain-of-function experiments indicate that in conscious mice, chemogenetic stimulation of either Phox2b^{LC} here, or Phox2b-expressing NTS neurons in our recent study [10], considerably increased basal ventilation *via* an RF increase, consistent with the prior report

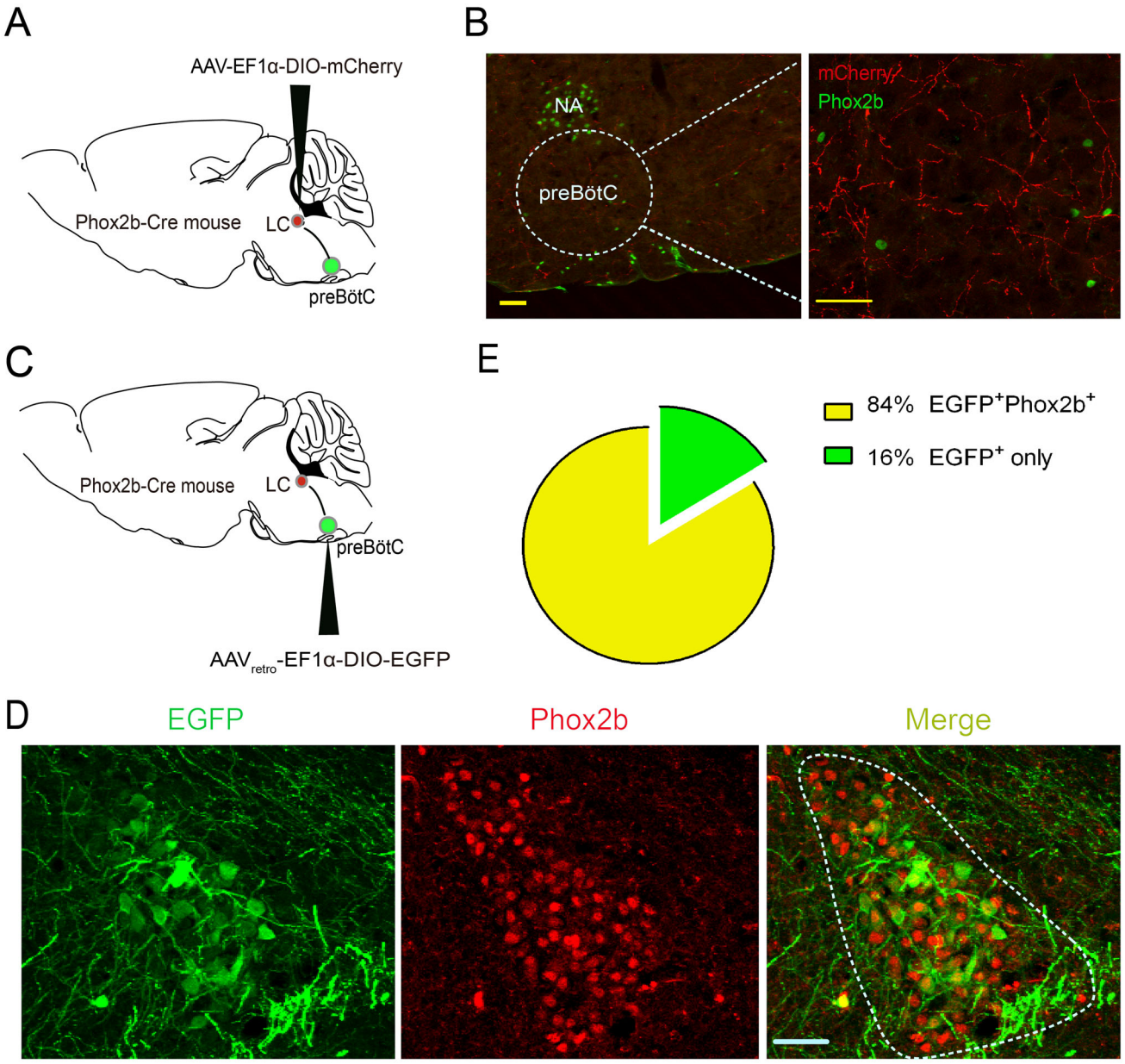

Fig. 8 Projection of Phox2b^{LC} neurons to the preBötC. **A** Schematic of anterograde virus injection into the LC of Phox2b-Cre mice. **B** Photomicrographs showing that mCherry-labeled axons of Phox2b^{LC} neurons project to the preBötC region. Left: dashed line, contour of the preBötC; right: enlarged image showing Phox2b-labeled NA and RTN neurons (green). Scale bars, 50 μm. **C** Schematic of retrograde virus injection into the preBötC in Phox2b-Cre mice. **D** Confocal images showing the cell bodies of EGFP-expressing neurons in the LC, most of which are Phox2b^{+}. **E** Cell counts showing that > 84% of EGFP neurons (n = 9 mice) projecting to the preBötC are Phox2b^{+} (scale bars, 50 μm).

demonstrating that RF is dramatically increased by photostimulation of Phox2b-expressing hindbrain neurons in a neonatal hindbrain–spinal cord preparation [32]. In these experiments, the basal MV increased *via* RF rather than TV, reflecting that at rest the RF appears to be the initial factor of respiratory mobilization, in line with the concept that the mobilization of RF is least costly in humans at rest [33]. Actually, the breathing pattern at rest has evolved to be a very economical mechanism, producing adequate ventilation at minimal cost. It has also been proposed that metabolic/chemical stimuli (e.g. hypercapnia and hypoxia) normally result in an increase in both RF and TV [34], as also supported by our present and prior findings [10, 11]. Although some studies have proposed the concept of differential control of RF and TV when challenged by different stressors [35], the underlying mechanism remains to be thoroughly investigated.

Ablation of Phox2b^{LC} Neurons Reduces the HCVR

The central respiratory chemoreflex is a crucial homeostatic mechanism to maintain normal blood gases [36]. Several studies have shown that the LC contains chemosensitive neurons that are recruited to mediate the ventilatory response to CO_2/H^+ [3, 23, 37]. For instance, proportional lesioning of LC noradrenergic neurons significantly blunts the HCVR *via* either a reduced TV [15] or RF [16]. Similar to these studies, our findings also demonstrated that selective lesioning of Phox2b^{LC} neurons, a subgroup of LC noradrenergic neurons, markedly attenuated the HCVR, primarily *via* a decreased TV. In addition, when destroying Phox2b-expressing neurons from any of the RTN, NTS, and LC, the HCVR was significantly reduced, strongly suggesting that a subgroup or most of the Phox2b-expressing neurons in these three regions are central chemoreceptor. Moreover, the basal ventilation remained unchanged, suggesting that when the central respiratory chemoreceptors from any of the RTN, NTS and LC were chemically or genetically lesioned, the remaining two centers most likely were able to compensate for the impaired respiratory function.

The HCVR largely relies on the normal function of central respiratory chemoreceptors. The molecular CO_2/H^+ sensors of central respiratory chemoreceptors differ in different brainstem regions. In the RTN, Phox2b-expressing neurons regulate breathing *via* recruiting TASK-2 channels and G-protein-coupled receptor 4 to sense the pH change [38]. In the NTS, acid-sensitive ion channels and background K^+ channels are suggested to mediate the pH-sensitive responses of Phox2b-expressing neurons *in vitro* [11]. Several studies have proposed that the chemosensitivity of LC neurons is mediated by different ion channels, including large conductance Ca^{2+}-activated K^+ channels [39], 4-aminopyridine-sensitive channels [40], and L-type Ca^{2+} channels [41]. In the present study, a small proportion of Phox2b^{LC} neurons was activated by CO_2, in support of the contribution of these neurons to the HCVR. However, we did not provide the ionic mechanism underlying the CO_2 sensitivity of Phox2b^{LC} neurons. Note that the pH-sensitive Phox2b^{LC} neurons may not contribute to the HCVR. Although the overwhelming number of LC neurons are TH-positive, actually these neurons may belong to different subsets that are responsible for different physiological functions.

The LC–preBötC Pathway

Metabolic regulation of breathing is mainly dependent on respiratory chemoreceptors, which are important for maintaining O_2 and CO_2 homeostasis, particularly during sleep [3, 42]. It has been proposed that central respiratory chemoreceptors provide an excitatory drive for the rCPG that is responsible for generating the eupneic rhythm. For example, the preBötC has been shown to receive direct synaptic transmission from RTN and NTS neurons [27, 43]; moreover, LC neurons have extensive connections with breathing-related brain regions, such as the NTS [44], parabrachial nucleus [45], and dorsal raphe nuclei [46], as well as the preBötC [13]. In the present study, we revealed the anatomical and functional relationships between Phox2b^{LC} neurons and the preBötC. Anatomically, both anterograde and retrograde viral tracing supported the conclusion that there is a direct projection of Phox2b^{LC} neurons to the preBötC. Functionally, stimulation of Phox2b^{LC} neurons enhanced the activity of putative preBötC neurons according to cFos analysis. Note that in the present study, cFos-labeled neurons in the preBötC region were anatomically defined. These neurons may not be responsible for the inspiratory rhythm and need to be functionally identified using *in vivo* or *in vitro* electrophysiological approaches. In addition, due to a lack of adequately specific markers of the breathing-related preBötC neurons, only cFos labeling was used here. These results reveal a circuit mechanism of the present gain-of-function and loss-of-function outcomes.

The LC has been implicated in attention, arousal, and panic/anxiety, and LC neuronal activity is highly state-dependent [47]. Taking these into account, some portion of the effect of Phox2b^{LC} neuron stimulation on ventilatory responses may well be directly through the LC-preBötC pathway, but another portion probably resulted from the consequence of behavioral arousal, suggesting an additive respiratory effect. In addition, exposure to CO_2 may not only increase pulmonary ventilation but also generate hypercapnia-elicited arousal [48] and a robust fear response in terms of behavior in mice, and panic symptom ratings in healthy volunteers and panic disorder patients [49]. Hence, some portion of the effect of ablation of Phox2b^{LC} neurons on the HCVR may be ascribed to the reduced respiratory drive to the preBötC due to the loss of pH-sensitive LC neurons, but another portion is likely due to the inhibition of hypercapnia-induced behavioral arousal or fear/panic. Based on the above analysis, in addition to the proposed LC–preBötC pathway to interpret the present results, other possible circuit mechanisms remain to be revealed.

Clinical Relevance and Conclusion

Heterozygous mutation of Phox2b is the leading cause of CCHS. One of the most important issues is to address the physiological role of Phox2b-containing cells. Interestingly, selective stimulation of Phox2b-expressing neurons from the RTN, NTS, and LC activates breathing in both

conscious and anesthetized mice, while ablation of these neurons significantly attenuates the central respiratory chemoreflex. These results shed light on the etiological mechanism underlying CCHS, and meanwhile provide central targets for potential clinical intervention. On the other hand, in addition to sustaining life, breathing may influence high-order behavior and thinking. For example, the LC–preBötC pathway contributes to the regulation of calm and arousal behaviors [13]. The present findings suggest that the effect of LC on breathing may also influence high-order behavior, but this awaits to be addressed.

In summary, the present study reveals that chemogenetic stimulation of $Phox2b^{LC}$ neurons increases basal pulmonary ventilation. In addition, a group of these neurons are required for the HCVR. The LC–preBötC pathway, as a circuit mechanism, is responsible for the control of breathing by $Phox2b^{LC}$ neurons. These findings help to better understand the pathogenic mechanisms underlying sleep-related hypoventilation or apnea.

Acknowledgements This work was supported by the National Natural Science Foundation of China (31971058 and 31571174), and the Youth Fund for Scientific and Technological Research in Higher Education Institutions of Hebei Province (QN2019019) and the Youth Science and Technology Talent Support Program of Natural Science in Hebei Medical University (CYQD201907).

Conflict of interest The authors claim that there are no conflicts of interest.

References

1. Zaidi S, Gandhi J, Vatsia S, Smith NL, Khan SA. Congenital central hypoventilation syndrome: An overview of etiopathogenesis, associated pathologies, clinical presentation, and management. Auton Neurosci 2018, 210: 1–9.
2. Moreira TS, Takakura AC, Czeisler C, Otero JJ. Respiratory and autonomic dysfunction in congenital central hypoventilation syndrome. J Neurophysiol 2016, 116: 742–752.
3. Guyenet PG, Stornetta RL, Bayliss DA. Central respiratory chemoreception. J Comp Neurol 2010, 518: 3883–3906.
4. Ramanantsoa N, Gallego J. Congenital central hypoventilation syndrome. Respir Physiol Neurobiol 2013, 189: 272–279.
5. Hernandez-Miranda LR, Ibrahim DM, Ruffault PL, Larrosa M, Balueva K, Muller T, *et al.* Mutation in LBX1/Lbx1 precludes transcription factor cooperativity and causes congenital hypoventilation in humans and mice. Proc Natl Acad Sci U S A 2018, 115: 13021–13026.
6. Pattyn A, Morin X, Cremer H, Goridis C, Brunet JF. The homeobox gene Phox2b is essential for the development of autonomic neural crest derivatives. Nature 1999, 399: 366–370.
7. Abbott SB, Stornetta RL, Fortuna MG, Depuy SD, West GH, Harris TE, *et al.* Photostimulation of retrotrapezoid nucleus phox2b-expressing neurons *in vivo* produces long-lasting activation of breathing in rats. J Neurosci 2009, 29: 5806–5819.
8. Takakura AC, Moreira TS, Stornetta RL, West GH, Gwilt JM, Guyenet PG. Selective lesion of retrotrapezoid Phox2b-expressing neurons raises the apnoeic threshold in rats. J Physiol 2008, 586: 2975–2991.
9. Wang S, Shi Y, Shu S, Guyenet PG, Bayliss DA. Phox2b-expressing retrotrapezoid neurons are intrinsically responsive to H^+ and CO_2. J Neurosci 2013, 33: 7756–7761.
10. Fu C, Shi L, Wei Z, Yu H, Hao Y, Tian Y, *et al.* Activation of Phox2b-expressing neurons in the nucleus tractus solitarii drives breathing in mice. J Neurosci 2019, 39: 2837–2846.
11. Fu C, Xue J, Wang R, Chen J, Ma L, Liu Y, *et al.* Chemosensitive Phox2b-expressing neurons are crucial for hypercapnic ventilatory response in the nucleus tractus solitarius. J Physiol 2017, 595: 4973–4989.
12. Carter ME, Yizhar O, Chikahisa S, Nguyen H, Adamantidis A, Nishino S, *et al.* Tuning arousal with optogenetic modulation of locus coeruleus neurons. Nat Neurosci 2010, 13: 1526–1533.
13. Yackle K, Schwarz LA, Kam K, Sorokin JM, Huguenard JR, Feldman JL, *et al.* Breathing control center neurons that promote arousal in mice. Science 2017, 355: 1411–1415.
14. Li L, Feng X, Zhou Z, Zhang H, Shi Q, Lei Z, *et al.* Stress accelerates defensive responses to looming in mice and involves a locus coeruleus-superior colliculus projection. Curr Biol 2018, 28: 859–871.e855.
15. Biancardi V, Bicego KC, Almeida MC, Gargaglioni LH. Locus coeruleus noradrenergic neurons and CO_2 drive to breathing. Pflugers Arch 2008, 455: 1119–1128.
16. Li A, Nattie E. Catecholamine neurones in rats modulate sleep, breathing, central chemoreception and breathing variability. J Physiol 2006, 570: 385–396.
17. Nobuta H, Cilio MR, Danhaive O, Tsai HH, Tupal S, Chang SM, *et al.* Dysregulation of locus coeruleus development in congenital central hypoventilation syndrome. Acta Neuropathol 2015, 130: 171–183.
18. Harper RM, Kumar R, Macey PM, Harper RK, Ogren JA. Impaired neural structure and function contributing to autonomic symptoms in congenital central hypoventilation syndrome. Front Neurosci 2015, 9: 415.
19. Paxinos G, Watson G. The Mouse Brain in Stereotaxic Coordinates. 2th ed. San Diego: Academic Press, 2001:124–129.
20. Berridge CW, Waterhouse BD. The locus coeruleus-noradrenergic system: modulation of behavioral state and state-dependent cognitive processes. Brain Res Brain Res Rev 2003, 42: 33–84.
21. Lazarenko RM, Milner TA, Depuy SD, Stornetta RL, West GH, Kievits JA, *et al.* Acid sensitivity and ultrastructure of the retrotrapezoid nucleus in Phox2b-EGFP transgenic mice. J Comp Neurol 2009, 517: 69–86.
22. Gomez JL, Bonaventura J, Lesniak W, Mathews WB, Sysa-Shah P, Rodriguez LA, *et al.* Chemogenetics revealed: DREADD occupancy and activation *via* converted clozapine. Science 2017, 357: 503–507.
23. Gargaglioni LH, Hartzler LK, Putnam RW. The locus coeruleus and central chemosensitivity. Respir Physiol Neurobiol 2010, 173: 264–273.
24. Zhao Z, Wang L, Gao W, Hu F, Zhang J, Ren Y, *et al.* A central catecholaminergic circuit controls blood glucose levels during stress. Neuron 2017, 95: 138–152 e5.
25. Del Negro CA, Funk GD, Feldman JL. Breathing matters. Nat Rev Neurosci 2018, 19: 351–367.
26. Guyenet PG. Regulation of breathing and autonomic outflows by chemoreceptors. Compr Physiol 2014, 4: 1511–1562.
27. Feldman JL, Del Negro CA, Gray PA. Understanding the rhythm of breathing: so near, yet so far. Annu Rev Physiol 2013, 75: 423–452.
28. Zhao F, Jiang HF, Zeng WB, Shu Y, Luo MH, Duan S. Anterograde trans-synaptic tagging mediated by adeno-associated virus. Neurosci Bull 2017, 33: 348–350.

29. Fan Y, Chen P, Raza MU, Szebeni A, Szebeni K, Ordway GA, *et al.* Altered expression of Phox2 transcription factors in the locus coeruleus in major depressive disorder mimicked by chronic stress and corticosterone treatment *in vivo* and *in vitro*. Neuroscience 2018, 393: 123–137.
30. Kang BJ, Chang DA, Mackay DD, West GH, Moreira TS, Takakura AC, *et al.* Central nervous system distribution of the transcription factor Phox2b in the adult rat. J Comp Neurol 2007, 503: 627–641.
31. Fan Y, Huang J, Duffourc M, Kao RL, Ordway GA, Huang R, *et al.* Transcription factor Phox2 upregulates expression of norepinephrine transporter and dopamine beta-hydroxylase in adult rat brains. Neuroscience 2011, 192: 37–53.
32. Cregg JM, Chu KA, Dick TE, Landmesser LT, Silver J. Phasic inhibition as a mechanism for generation of rapid respiratory rhythms. Proc Natl Acad Sci U S A 2017, 114: 12815–12820.
33. Mead J. The control of respiratory frequency. Ann N Y Acad Sci 1963, 109: 724–729.
34. Nicolo A, Girardi M, Sacchetti M. Control of the depth and rate of breathing: metabolic vs. non-metabolic inputs. J Physiol 2017, 595: 6363–6364.
35. Tipton MJ, Harper A, Paton JFR, Costello JT. The human ventilatory response to stress: rate or depth? J Physiol 2017, 595: 5729–5752.
36. Guyenet PG, Bayliss DA. Neural control of breathing and CO_2 homeostasis. Neuron 2015, 87: 946–961.
37. Haxhiu MA, Yung K, Erokwu B, Cherniack NS. CO_2-induced c-fos expression in the CNS catecholaminergic neurons. Respir Physiol 1996, 105: 35–45.
38. Kumar NN, Velic A, Soliz J, Shi Y, Li K, Wang S, *et al.* PHYSIOLOGY. Regulation of breathing by CO_2 requires the proton-activated receptor GPR4 in retrotrapezoid nucleus neurons. Science 2015, 348: 1255–1260.
39. Imber AN, Patrone LGA, Li KY, Gargaglioni LH, Putnam RW. The role of Ca^{2+} and BK channels of locus coeruleus (LC) neurons as a brake to the CO_2 chemosensitivity response of rats. Neuroscience 2018, 381: 59–78.
40. Li KY, Putnam RW. Transient outwardly rectifying A currents are involved in the firing rate response to altered CO_2 in chemosensitive locus coeruleus neurons from neonatal rats. Am J Physiol Regul Integr Comp Physiol 2013, 305: R780–792.
41. Imber AN, Putnam RW. Postnatal development and activation of L-type Ca^{2+} currents in locus ceruleus neurons: implications for a role for Ca^{2+} in central chemosensitivity. J Appl Physiol (1985) 2012, 112: 1715–1726.
42. He C, Hu Z. Homeostasis of synapses: Expansion during wakefulness, contraction during sleep. Neurosci Bull 2017, 33: 359–360.
43. Li P, Janczewski WA, Yackle K, Kam K, Pagliardini S, Krasnow MA, *et al.* The peptidergic control circuit for sighing. Nature 2016, 530: 293–297.
44. Lopes LT, Patrone LG, Li KY, Imber AN, Graham CD, Gargaglioni LH, *et al.* Anatomical and functional connections between the locus coeruleus and the nucleus tractus solitarius in neonatal rats. Neuroscience 2016, 324: 446–468.
45. Arima Y, Yokota S, Fujitani M. Lateral parabrachial neurons innervate orexin neurons projecting to brainstem arousal areas in the rat. Sci Rep 2019, 9: 2830.
46. Uribe-Marino A, Angelica Castiblanco-Urbina M, Luciano Falconi-Sobrinho L, Dos Anjos-Garcia T, de Oliveira RC, Mendes-Gomes J, *et al.* The alpha- and beta-noradrenergic receptors blockade in the dorsal raphe nucleus impairs the panic-like response elaborated by medial hypothalamus neurons. Brain Res 2019: 146468.
47. Aston-Jones G, Bloom FE. Activity of norepinephrine-containing locus coeruleus neurons in behaving rats anticipates fluctuations in the sleep-waking cycle. J Neurosci 1981, 1: 876–886.
48. Aston-Jones G, Cohen JD. An integrative theory of locus coeruleus-norepinephrine function: adaptive gain and optimal performance. Annu Rev Neurosci 2005, 28: 403–450.
49. Leibold NK, van den Hove DL, Viechtbauer W, Buchanan GF, Goossens L, Lange I, *et al.* CO_2 exposure as translational cross-species experimental model for panic. Transl Psychiatry 2016, 6: e885.